Hyperbolic attractor in a system of coupled non-autonomous van der Pol oscillators: Numerical test for expanding and contracting cones

S.P. Kuznetsov and I.R. Sataev

April 10, 2007

Kotel'nikov Institute of Radio-Engineering and Electronics of RAS,
Saratov Branch, Zelenaya 38, 410019, Saratov, Russian Federation

Abstract

We present numerical verification of hyperbolic nature for chaotic attractor in a system of two coupled non-autonomous van der Pol oscillators (Kuznetsov, Phys. Rev. Lett., **95,** 144101, 2005). At certain parameter values, in the 4D phase space of the Poincaré map we indicate a toroidal domain (a direct product of a circle and a 3D ball), which is mapped into itself and contains the attractor we analyze. In accordance with the computations, in this absorbing domain the conditions of hyperbolicity are valid, which are formulated in terms of contracting and expanding cones in the vector spaces of the small state perturbations.

PACS: 05.45-a
Keywords: chaos; attractor; hyperbolicity; Smale – Williams solenoid

Mathematical theory of chaotic dynamics based on a rigorous axiomatic foundation exploits a concept of hyperbolicity [1-8]. In hyperbolic attractors all trajectories are of saddle type; their stable and unstable manifolds are of the same dimension, and there are no tangencies between the stable and unstable manifolds. These attractors possess strong chaotic properties, like existence of the well-defined invariant measure of Sinai–Bowen–Ruelle, a possibility of description in terms of Markov partitions and symbolic dynamics, positive metric and topological entropy etc. Such hyperbolic (or, more definitely, *uniformly hyperbolic*) attractors are robust or structurally stable, that means insensitivity of the type of dynamics and of the phase space structure in respect to slight variations of functions and parameters in the evolutionary equations.

In textbooks and reviews on nonlinear dynamics, such attractors are represented by artificial mathematical constructions, like Plykin attractor and Smale – Williams solenoid [1-8]. For realistic systems, in which the chaotic dynamics is mathematically proved, like the Lorenz model [9,10], the strange attractors do not relate to the class of uniformly hyperbolic (not all axiomatic statements of the classic hyperbolic theory are valid for them).

We are aware of a few works, which discuss examples of true hyperbolic dynamics in systems governed by differential equations. One relates to a mechanical system called triple linkage, which allows description in terms of motion on a surface of negative curvature in a frictionless case. In presence of dissipation and feedback, it is expected to manifest a hyperbolic chaotic attractor [11, 12]. In Ref. [12] the author constructs an artificial 3D flow system with a Plykin type attractor in the Poincaré map. This example definitely looks too complicated to be realizible as a physical device. In Ref. [13] the authors argue in favor of existence of an attractor of Plykin type in a flow system motivated by neural dynamics. Finally, in this context it is worth noting a paper [14] discussing a possible bifurcation mechanism of the birth of hyperbolic attractors.

In a recent paper of one of the authors [15], an idea was advanced of implementation of a hyperbolic attractor in a system of two coupled non-autonomous van der Pol oscillators. In the Poincaré map a chaotic attractor has been found, which demonstrates some characteristic signs of hyperbolic attractors. By a nature of transformation of the phase space volume in the course of the evolution, it is similar to the Smale – Williams solenoid. It looks robust: the Cantor-like transverse structure and the positive Lyapunov exponent are insensitive to variation of parameters in the equations. An analogous system has been built as an electronic device and studied in experiment [16].

Obviously, it would be desirable to have a mathematical confirmation of the hyperbolic nature of the attractor. As Sinai has suggested in due time [1], one possible way for substantiation of the hyperbolicity for attractor of a Poincaré map consists in numerical verification of certain sufficient conditions formulated in terms of inclusions for expanding and contracting cones in tangent vector space (the space of small perturbation vectors). In this paper, we discuss a method and present results of computer verification of these conditions in application to the system of coupled non-autonomous van der Pol oscillators.

The system proposed in Ref. [15] is represented by a set of differential equations

$$\begin{array}{ll} \dot{x} = \omega_0 u, & \dot{u} = -\omega_0 x + [A\cos(2\pi t/T) - x^2]u + (\varepsilon/\omega_0) y \cos\omega_0 t, \\ \dot{y} = 2\omega_0 v, & \dot{v} = -2\omega_0 y + [-A\cos(2\pi t/T) - y^2]v + (\varepsilon/2\omega_0) x^2. \end{array} \qquad (1)$$

The system consists of two van der Pol oscillators with characteristic frequencies ω_0 and $2\omega_0$. Here x and u represent coordinate and velocity for the first oscillator, and y and v for the second one. In each subsystem the parameter responsible for the birth of the limit cycle, is forced to oscillate slowly with period T and amplitude A. The

parameter modulation is of opposite phase, and the subsystems become active turn by turn, each on its own half-period T. The coupling is characterized by parameter ε. The first oscillator affects the second one via a quadratic term in the equation. The backward coupling is introduced by a product of the variable y and an auxiliary signal of frequency ω_0. It is assumed that the interval T contains an integer number of periods of the auxiliary signal $N_0 = \omega_0 T/2\pi$, so the external driving is periodic.

Beside the basic equations, we write down a set of equations for small perturbations evolving along the given trajectory needed both for the procedure of verification of hyperbolicity and calculation of the Lyapunov exponents. It reads

$$\begin{array}{ll} \delta\dot{x} = \omega_0\delta u, & \delta\dot{u} = -\omega_0\delta x - 2xu\delta x + [A\cos(2\pi t/T) - x^2]\delta u + (\varepsilon/\omega_0)\delta y\cos\omega_0 t, \\ \delta\dot{y} = 2\omega_0\delta v, & \delta\dot{v} = -2\omega_0\delta y - 2yv\delta y + [-A\cos(2\pi t/T) - y^2]\delta v + (\varepsilon/\omega_0)x\delta x. \end{array} \tag{2}$$

For a detailed study, we select

$$\omega_0 = 2\pi,\ T = 6,\ A = 5,\ \varepsilon = 0.5. \tag{3}$$

The system operates as follows. Let the phase of the first oscillator on an active stage be ψ: $x \propto \sin(\omega_0 t + \psi)$. As the half-period comes to the end, the excitation of the second oscillator occurs in presence of the term x^2 that serves as priming. This term contains the second harmonic: $\cos(2\omega_0 t + 2\psi)$, and its phase is 2ψ. Hence, the oscillations of y will get this phase 2ψ. Half a period later, excitation of the first oscillator is stimulated with the term $y\cos\omega_0 t$. Then, the oscillations of x accept the phase 2ψ from the second oscillator. On successive periods the phase of the first oscillator will follow approximately the equation

$$\psi_{n+1} = 2\psi_n + \text{const}\ \ (\text{mod}2\pi). \tag{4}$$

The relation (4) called the Bernoulli map is well known as one of the simplest model examples in the chaos theory.[1]

For accurate description of the discrete time dynamics it is convenient to turn to the Poincaré map [2-8, 17,18]. From solution of the differential equations (1) with the initial state $\mathbf{x}_n = \{x(t_n), u(t_n), y(t_n), v(t_n)\}$ at $t_n = nT$, we get a new vector $\mathbf{x}_{n+1}$ at $t_{n+1} = (n+1)T$. As it is determined uniquely by $\mathbf{x}_n$, we introduce a function that maps the 4D space $\{x, u, y, v\}$ into itself: $\mathbf{x}_{n+1} = \mathbf{T}(\mathbf{x}_n)$. This Poincaré map appears due to the evolution determined by the differential equations with smooth and

[1]The constant in Eq. (4) accounts a phase shift in the course of transfer of the excitation from one oscillator to another and may be removed by a shift of origin for the phase variable. We stress that the phase ψ cannot be defined globally on the whole time interval T: it has sense only in the context of the discrete time description. Indeed, on the stage when the first oscillator is damped, its amplitude is small, and the phase is not well defined.

bounded right-hand parts in a finite domain of variables $\{x, u, y, v\}$. In accordance with theorems of existence, uniqueness, continuity, and differentiability of solutions of differential equations, the map $\mathbf{T}$ is a diffeomorphism, a one-to-one differentiable map of class C^∞ [17].

Hereafter, we will deal always with the discrete-time description of the dynamics in terms of the Poincaré map.

In the course of iterations of the map $\mathbf{x}_{n+1} = \mathbf{T}(\mathbf{x}_n)$, a small phase-space volume is stretched locally in a direction associated with the phase in the approximate equation (4) and undergoes contraction in the other three directions. To interpret the mapping geometrically, imagine a solid toroid (a direct product of a circle and a 3D ball) in the 4D space. One iteration of the Poincaré map will correspond to longitudinal stretch and transversal contraction of the toroid with subsequent insertion of the doubly folded "tube" into the original domain. It is analogous to the construction of Smale and Williams with the only difference that we deal with the 4D rather than the 3D phase space.

The mentioned toroid will be referred to as an absorbing domain U. It means that under application of the map $\mathbf{T}$ the images of all points from U will belong to its interior: $\mathbf{T}(U) \subset \operatorname{Int} U$. The attractor then may be defined as intersection of the images obtained under multiple action of the map: $A = \bigcap_{n=1}^{\infty} \mathbf{T}^n(U)$.

To write down an analytic definition for the domain U it is convenient to redefine the coordinate system. We introduce new variables $\{x_0, x_1, x_2, x_3\}$ as follows:

$$x_0 = x/r_0, \quad x_1 = (u - c_{ux}x)/r_1, \quad x_2 = y - c_{yx}x - c_{yu}u, \quad x_3 = v - c_{vx}x - c_{vu}u - c_{vy}y. \tag{5}$$

To determine the constants we accumulate a large number of points $\{x, u, y, v\}$ on the attractor in the Poincaré section by numerical solution of the equations (1). Then, by the least square method we find out the coefficients to minimize the mean-square values $< (u - c_{ux}x)^2 >$, $< (y - c_{yx}x - c_{yu}u)^2 >$, $< (v - c_{vx}x - c_{vu}u - c_{vy}y)^2 >$. Geometrically, it corresponds to directing the coordinate axes along the principal axes of the ellipsoid that approximates the attractor. Additionally, we normalize x_0 and x_1 by appropriate factors to have $<x_0^2>=<x_1^2>\approx 1/2$. Finally, at the parameter set (3) we get

$$\begin{aligned} &c_{ux} = 0.438, \;\; c_{yx} = -0.042, \;\; c_{yu} = 0.226, \;\; c_{vx} = -0.218, \\ &c_{vu} = 0.029, \;\; c_{vy} = -0.118, \;\; r_0 = 0.812, \quad r_1 = 0.721. \end{aligned} \tag{6}$$

In the new coordinates, let us define the absorbing domain U by the inequality:

$$\left[\left(\sqrt{x_0^2 + x_1^2} - r\right)/d_r\right]^2 + (x_2/d)^2 + (x_3/d)^2 \leq 1. \tag{7}$$

Empirically selected constants are $r = 0.94, \;\; d_r = 0.4, \;\; d = 0.15$.

In Fig.1 we show a 3D plot illustrating mutual location of the domains U and $\mathbf{T}(U)$. It is in obvious correspondence with the first step of the construction of the Smale – Williams attractor. The transformed domain $\mathbf{T}(U)$ looks like a narrow band because of very strong compression of the phase volume in the respective directions.

We will verify hyperbolicity conditions required by a theorem (see e.g. [1, 5, 12]) adopted for the problem under consideration. Unlike the general formulation, it is sufficient here to deal with a diffeomorphism of class C^∞ in the Euclidian space $\mathbb{R}^4$, namely, the Poincaré map $\mathbf{T}(\mathbf{x})$. Evolution of a perturbed state $\mathbf{x}+\delta\mathbf{x}$ corresponds to transformation of the perturbation vector $\delta\mathbf{x}$ in linear approximation $\delta\mathbf{x}' = \mathbf{DT}_\mathbf{x}\delta\mathbf{x}$, where $\mathbf{DT}_\mathbf{x}$ is the Jacobi matrix at $\mathbf{x}$: $\mathbf{DT}_\mathbf{x} = \{\partial x_i'/\partial x_j\}$, $i, j = 0, 1, 2, 3$. The notion $\mathbf{DT}_\mathbf{x}^{-1}$ designates the derivative matrix for the inverse mapping $\mathbf{T}^{-1}(\mathbf{x})$.

Theorem [1,5,12]. Suppose that a diffeomorphism $\mathbf{T}$ of class C^∞ maps a bounded domain $U \subset \mathbb{R}^4$ into itself: $\mathbf{T}(U) \subset \mathrm{Int}\, U$, and $A \subset \mathrm{Int}\, U$ is an invariant subset for the diffeomorphism. The set A will be uniformly hyperbolic if there exists a constant $\gamma > 1$ and the following conditions hold:

1. For each $\mathbf{x} \in A$ in the space $\mathbb{V}_x$ of 4D vectors $\delta\mathbf{x}$ the expanding and contracting cones $S_\mathbf{x}^\gamma$ and $C_\mathbf{x}^\gamma$ may be defined, such that $\|\mathbf{DT}_\mathbf{x}\mathbf{u}\| > \gamma\|\mathbf{u}\|$ for all $\mathbf{u} \in S_\mathbf{x}^\gamma$, and $\left\|\mathbf{DT}_\mathbf{x}^{-1}\mathbf{v}\right\| > \gamma\|\mathbf{v}\|$ for all $\mathbf{v} \in C_\mathbf{x}^\gamma$; moreover, for all $\mathbf{x} \in A$ they satisfy $S_\mathbf{x}^\gamma \cap C_\mathbf{x}^\gamma = \emptyset$ and $S_\mathbf{x}^\gamma + C_\mathbf{x}^\gamma = \mathbb{V}_x$.

2. The cones $S_\mathbf{x}^\gamma$ are invariant in respect to action of $\mathbf{DT}$, and $C_\mathbf{x}^\gamma$ are invariant in respect to action of $\mathbf{DT}^{-1}$, i.e. for all $\mathbf{x} \in A$ $\mathbf{DT}_\mathbf{x}(S_\mathbf{x}^\gamma) \subset S_{\mathbf{T}(\mathbf{x})}^\gamma$ and $\mathbf{DT}_\mathbf{x}^{-1}(C_\mathbf{x}^\gamma) \subset C_{\mathbf{T}^{-1}(\mathbf{x})}^\gamma$.

If the formulated conditions are valid for a domain containing the attractor, say, $\mathbf{T}^n(U)$, they are obviously true for the attractor $A = \bigcap_{n=1}^{\infty} \mathbf{T}^n(U)$. The procedure of computer verification of these conditions consists in the following.

Starting at $\mathbf{x} = \{x_0, x_1, x_2, x_3\} \in U$, we perform numerical solution of Eqs. (1) on the interval $t \in [0, T]$ and get the image $\mathbf{x}' = \{x_0', x_1', x_2', x_3'\}$. In parallel, we solve the set of equations for small perturbations (2) over the same period. It is done for four times, assigning the initial vectors in coordinates (5) as follows: $\{\delta x_i\} = \{1,0,0,0\}, \{0,1,0,0\}, \{0,0,1,0\}$ and $\{0,0,0,1\}$. From the resulting four vector-columns we compose a matrix $\mathbf{U} = \mathbf{DT}_\mathbf{x}$.

After one iteration of the Poincaré map any initial perturbation vector $\mathbf{u}$ transforms to $\mathbf{u}' = \mathbf{U}\mathbf{u}$. A squared Euclidean norm of this vector is $\|\mathbf{u}'\|^2 = \mathbf{u}^T\mathbf{U}^T\mathbf{U}\mathbf{u}$, where T means the transposition. Via the inverse matrix $\mathbf{U}^{-1}$ we can write $\mathbf{u} = \mathbf{U}^{-1}\mathbf{u}'$ and $\|\mathbf{u}\|^2 = \mathbf{u}'^T\mathbf{U}^{-1,T}\mathbf{U}^{-1}\mathbf{u}'$. A condition that preimage of $\mathbf{u}'$ relates to the expanding cone $S_\mathbf{x}^\gamma$, is an inequality $\|\mathbf{u}'\| > \gamma\|\mathbf{u}\|$, or $\mathbf{u}'^T\mathbf{H}_\gamma\mathbf{u}' < 0$, where $\mathbf{H}_\gamma = \mathbf{U}^{-1,T}\mathbf{U}^{-1} - \gamma^{-2}$.

Starting at $\mathbf{x}' = \mathbf{T}(\mathbf{x}) = \{x'_0, x'_1, x'_2, x'_3\}$, a vector $\mathbf{u}'$ transforms to $\mathbf{u}'' = \mathbf{U}'\mathbf{u}'$, and we have $\|\mathbf{u}''\|^2 = \mathbf{u}'^T\mathbf{U}'^T\mathbf{U}'\mathbf{u}'$. The expanding cone $S^\gamma_{\mathbf{T}(\mathbf{x})}$ at $\mathbf{x}' = \mathbf{T}(\mathbf{x})$ is determined by an inequality $\|\mathbf{u}''\| > \gamma\|\mathbf{u}'\|$, or $\mathbf{u}'^T\mathbf{H}'_\gamma\mathbf{u}' > 0$, where $\mathbf{H}'_\gamma = \mathbf{U}^T\mathbf{U} - \gamma^2$.

Thus, the required condition $\mathbf{DT}_\mathbf{x}(S^\gamma_\mathbf{x}) \subset S^\gamma_{\mathbf{T}(\mathbf{x})}$ is formulated in terms of two quadratic forms: If the inequality $\mathbf{u}'^T\mathbf{H}_\gamma\mathbf{u}' < 0$ holds, then the inequality $\mathbf{u}'^T\mathbf{H}'_\gamma\mathbf{u}' > 0$ must be valid too.

Let us perform a canonical reduction of the quadratic form $\mathbf{u}'^T\mathbf{H}'_\gamma\mathbf{u}'$ by a coordinate change. As the matrix $\mathbf{U}'^T\mathbf{U}'$ is positive definite, an orthonormal basis of eigenvectors $\mathbf{d}_0, \mathbf{d}_1, \mathbf{d}_2, \mathbf{d}_3$ may be chosen. Then, the matrix $\mathbf{D} = (\mathbf{d}_0, \mathbf{d}_1, \mathbf{d}_2, \mathbf{d}_3)$ is a diagonalizer: $\mathbf{D}^T\mathbf{U}'^T\mathbf{U}'\mathbf{D} = \{\Lambda_i^2\delta_{ij}\}$, $i, j = 0, 1, 2, 3$. The eigenvalues on the diagonal Λ_i^2 are supposed to be arranged in the decreasing order. In our case, there will be one stretching and three contracting directions, so, $\Lambda_0^2 > 1$, $\Lambda_{1,2,3}^2 < 1$. Let γ be selected in such way that $\Lambda_0^2 > \gamma^2$, $\Lambda_{1,2,3}^2 < \gamma^2$. Under the transformation $\mathbf{D}$ the matrix $\mathbf{H}'_\gamma$ becomes diagonal too: $\tilde{\mathbf{H}}'_\gamma = \mathbf{D}^T\mathbf{H}'_\gamma\mathbf{D} = \mathbf{D}^T(\mathbf{U}'^T\mathbf{U}' - \gamma^2)\mathbf{D} = \{(\Lambda_i^2 - \gamma^2)\delta_{ij}\}$; here one diagonal element is positive, and others are negative.[2] By the additional dilatation (compression) $\mathbf{S} = \{s_i^{-1}\delta_{ij}\}$, $s_0 = \sqrt{\Lambda_0^2 - \gamma^2}$, $s_{1,2,3} = \sqrt{\gamma^2 - \Lambda_{1,2,3}^2}$, we get $\hat{\mathbf{H}}'_\gamma = \mathbf{S}^T\mathbf{D}^T(\mathbf{U}^T\mathbf{U} - \gamma^2)\mathbf{DS} = \sigma_i\delta_{ij}$, $\sigma_0 = 1$, $\sigma_{1,2,3} = -1$. The same transformations applied to the matrix $\mathbf{H}_\gamma = \mathbf{U}^{-1,T}\mathbf{U}^{-1} - \gamma^{-2}$ yield $\hat{\mathbf{H}}_\gamma = \mathbf{S}^T\mathbf{D}^T(\mathbf{U}^{-1,T}\mathbf{U}^{-1} - \gamma^{-2})\mathbf{DS} = \{h_{ij}\}$, where $h_{ij} = h_{ji}$.

A condition for vector $\mathbf{c}=\{1,c_1,c_2,c_3\}$ to belong to the expanding cone $S^\gamma_{\mathbf{T}(\mathbf{x})}$ is $\mathbf{c}^T\hat{\mathbf{H}}'\mathbf{c} > 0$, or

$$c_1^2 + c_2^2 + c_3^2 < 1. \tag{8}$$

In the 3D space $\{c_1,c_2,c_3\}$ this corresponds to interior of the unit ball.

A condition that preimage of the vector $\mathbf{c}=\{1,c_1,c_2,c_3\}$ belongs to the expanding cone at $\mathbf{x}$ is $\mathbf{c}^T\hat{\mathbf{H}}_\gamma\mathbf{c} < 0$, or $h_{00} + \sum\limits_{\alpha=1}^{3}(h_{0\alpha}c_\alpha + h_{\alpha 0}c_\alpha) + \sum\limits_{\alpha,\beta=1}^{3} h_{\alpha\beta}c_\alpha c_\beta < 0$. In the space $\{c_1,c_2,c_3\}$ this relation determines the interior of a certain ellipsoid. The inclusion $\mathbf{DT}_\mathbf{x}(S^\gamma_\mathbf{x}) \subset S^\gamma_{\mathbf{T}(\mathbf{x})}$ will be fulfilled, if the ellipsoid is placed inside the unit ball. Let us formulate an inequality sufficient to ensure such a disposition. We can evaluate coordinates for the center of the ellipsoid from a set of linear algebraic equations

$$\sum_{\beta=1}^{3} h_{\alpha\beta}\bar{c}_\beta = -h_{\alpha 0}, \quad \alpha = 1, 2, 3, \tag{9}$$

[2]This property is checked in the course of computations at each analyzed point of the absorbing domain naturally: its violation would entail a non-correct operation of taking a square root of a negative number. The inequalities for eigenvalues of the matrix $\mathbf{U}_\mathbf{x}^T\mathbf{U}_\mathbf{x}$ ensure fulfillment of the condition that a sum of subsets of the linear vector space (that is a set of all possible linear combinations of vectors from the expanding and contracting cones) is the full 4D vector space: $S^\gamma_\mathbf{x} + C^\gamma_\mathbf{x} = \mathbb{V}$.

and then estimate a distance of this point from the center of the unit ball: $\rho = \sqrt{\bar{c}_1^2 + \bar{c}_2^2 + \bar{c}_3^2}$. With transfer of the origin to the point $\{\bar{c}_1,\ \bar{c}_2,\ \bar{c}_3\}$, the equation of the ellipsoid surface becomes $\sum_{\alpha,\beta=1}^{3} h_{\alpha\beta}\tilde{c}_\alpha\tilde{c}_\beta = R^2$, where $\tilde{c}_\alpha = c_\alpha - \bar{c}_\alpha$, and $R^2 = -h_{00} - \sum_{\alpha=1}^{3}(h_{0\alpha}\bar{c}_\alpha + h_{\alpha 0}\bar{c}_\alpha) - \sum_{\alpha,\beta=1}^{3} h_{\alpha\beta}\bar{c}_\alpha\bar{c}_\beta$.

Now, consider a symmetric 3×3 matrix $\mathbf{h} = \{h_{\alpha\beta}\}$. In diagonal representation obtained with a certain coordinate transformation $(\tilde{c}_1, \tilde{c}_2, \tilde{c}_3) \to (\xi_1, \xi_2, \xi_3)$, the equation for the ellipsoid surface takes a form $l_1\xi_1^2 + l_2\xi_2^2 + l_3\xi_3^2 = R^2$, where l_1, l_2, l_3 are eigenvalues of the matrix $\mathbf{h}$. The largest principal semiaxis of the ellipsoid is expressed via the smallest eigenvalue: $r_{\max} = R/\sqrt{l_{\min}}$. Now, an obvious sufficient condition for the ellipsoid to be positioned inside the unit ball is given by the inequality

$$r_{\max} + \rho < 1. \tag{10}$$

It completes the procedure of verification of the expanding cones inclusion for the point $\mathbf{x}$.

It may be shown that with $\gamma < 1$ application of the above procedure in U is equivalent to verification of the condition for contracting cones in the domain $\mathbf{T}^2(U)$ with parameter $\gamma' = 1/\gamma > 1$: $\mathbf{DT}_\mathbf{x}^{-1}(C_\mathbf{x}^{1/\gamma}) \subset C_{\mathbf{T}^{-1}(\mathbf{x})}^{1/\gamma}$. It is so because the cones S^γ and $C^{1/\gamma}$ are complimentary sets: $\bar{S}^\gamma \cup \bar{C}^{1/\gamma} = \mathbb{V}$. (Here S^γ with $\gamma < 1$ corresponds to the cone of vectors, which either expand, or contract, but no stronger than by the factor γ.) Hence, fulfillment of the inequality (10) checked inside U for two parameters γ and $1/\gamma$ would imply that both conditions for expanding and for contracting cones are valid in the domain $\mathbf{T}^2(U)$, which contains the attractor.[3] This is sufficient to draw a conclusion on the hyperbolic nature of the attractor.

For computer verification of the required inclusions, the Poincaré map and the Jacobi matrices were produced by means of joint numerical solution of the differential equations (1) and the linearized equations (2) on the time interval T. We used the Runge – Kutta method of the 8-th order based on formulas of Dormand and Prince with automatic selection of step (the accuracy for one step was assigned to be 10^{-11}) and an extrapolation method (the accuracy for one step assigned 10^{-15}) [19]. For solution of sets of linear algebraic equations, matrix diagonalization, and eigenvalue problem solving, we used sub-programs from the library LAPACK [20].

In accordance with performed computations, the eigenvalues of the matrix $\mathbf{U}^{\mathrm{T}}\mathbf{U} = (\mathbf{DT}_\mathbf{x})^T\mathbf{DT}_\mathbf{x}$ satisfy the conditions $\Lambda_0^2 > 1$ and $\Lambda_{1,2,3}^2 < 1$ in the entire absorbing domain U. The sufficient condition for inclusion of the cones $\mathbf{DT}_\mathbf{x}(S_\mathbf{x}^\gamma) \subset S_{\mathbf{T}(\mathbf{x})}^\gamma$ appears to be valid in the domain U at least in the interval $0.64 < \gamma^2 < 1.35$.

[3] For the same γ, the cones S^γ and C^γ have a common border only at $\gamma = 1$. With $\gamma > 1$ they do not intersect, as required by the Theorem condition: $S_\mathbf{x}^\gamma \cap C_\mathbf{x}^\gamma = \emptyset$.

To discuss details, let us consider a 3D hypersurface defined by an equation

$$\left[\left(\sqrt{x_0^2+x_1^2}-r\right)/d_r\right]^2+(x_2/d)^2+(x_3/d)^2=R^2. \tag{11}$$

At $R=1$ it is a border of the domain U; at $R<1$ it belongs to its interior. We can parametrize this hypersurface by three angle coordinates ϕ, ψ, and θ:

$$\begin{array}{ll} x_0=(Rd_r\cos\theta+r)\sin\psi, & x_1=(Rd_r\cos\theta+r)\cos\psi, \\ x_2=Rd\sin\theta\cos\phi, & x_3=Rd\sin\theta\sin\phi. \end{array} \tag{12}$$

The variable ψ may be regarded as a phase of the first oscillator at the Poincaré cross-section, and ϕ as a phase of the second oscillator at the same instant. Numerical computations on a 3D grid with step $2\pi/M$ at $M=50$ show that at a fixed R the eigenvalues $\mathbf{U}^{\mathrm{T}}\mathbf{U}$ and the value $r_{\max}+\rho=f(R,\phi,\psi,\theta)$ depend essentially on ψ and θ, while the dependence on ϕ is very weak. In Fig. 2 we present a plot of the eigenvalues Λ_0^2 and Λ_1^2 versus two angle variables at fixed $\phi=0.46$ on a border of the absorbing domain. Observe that Λ_0^2 is always larger than 1, and Λ_1^2 is always less than 1 (the same is true, naturally, for $\Lambda_{2,3}^2$). To be sure in validity of the mentioned relations in the entire domain U we computed the global minimum of Λ_0^2 and the global maximum of Λ_1^2 over the angle variables, and then traced their dependences on R (see panel (b)). As found, $\min\limits_{\mathbf{x}\in U}\Lambda_0^2\approx 2.258>1$ and $\max\limits_{\mathbf{x}\in U}\Lambda_1^2\approx 0.532<1$.

Now, we turn to the condition of the cones inclusion.

On the plot of the function $f=\rho+r_{max}$ at $\gamma^2=1.1$ one global maximum can be seen of a value varied in dependence on ϕ and R. At $R=1$ and some ϕ the maximum reaches $f_{max}\approx$0.929441 (that corresponds to a point M on the border of the domain U with coordinates $x_0=-0.102628$, $x_1=-0.544957$, $x_2=0.000581$, $x_3=0.040066$), but remains definitely less than 1, see Fig. 3. Panel (b) illustrates mutual disposition for the cones $\mathbf{DT}_{\mathbf{x}}(S_{\mathbf{x}}^{\gamma})$ and $S_{\mathbf{T(x)}}^{\gamma}$ at the point M. The plot shows a 3D cross-section of the 4D vector space $\mathbb{V}_{\mathbf{T(x)}}$ by a hyperplane orthogonal to the expanding direction. The coordinate axes on the plot correspond to the principal semiaxes of the ellipsoid representing the cross-section of the cone $S_{\mathbf{T(x)}}^{\gamma}$. Due to scale selection it looks like a ball. The ellipsoid representing the cross-section of $\mathbf{DT}_{\mathbf{x}}(S_{\mathbf{x}}^{\gamma})$ looks like a narrow "needle", because of strong phase volume compression in two directions. Its disposition inside the large ball means validity of the condition $\mathbf{DT}_{\mathbf{x}}(S_{\mathbf{x}}^{\gamma})\subset S_{\mathbf{T(x)}}^{\gamma}$. The ball circumscribed around the ellipsoid is posed inside the large ball too; that expresses the sufficient condition (10). For smaller R the global maximum of $r_{\max}+\rho$ only decreases (Fig. 4a). Analogous computations with other values of γ indicate that the required inclusions for the cones S take place at least in the interval $0.64<\gamma^2<1.35$ (Fig. 4b). As explained, the correctness of the checked condition with $\gamma<1$ implies validity of the condition for the contracting cones $\mathbf{DT}_{\mathbf{x}}^{-1}(C_{\mathbf{x}}^{1/\gamma})\subset C_{\mathbf{T}^{-1}(\mathbf{x})}^{1/\gamma}$ in the domain $\mathbf{T}^2(U)$. We

conclude that in $\mathbf{T}^2(U)$, both conditions for expanding and contracting cones are true, say, at $\gamma^2 = 1.1$. Hence, the analyzed attractor is uniformly hyperbolic. This assertion, although not proven in a classic mathematical style, follows with definiteness from the Theorem, conditions of which have been checked in the computations. Assuming the hyperbolicity established, let us illustrate now some attributes of the hyperbolic dynamics.

To start, we note that dynamics on the attractor is chaotic. In the course of time evolution, both oscillators become active turn-by-turn, passing the excitation one to another. Figure 5 shows typical plots for x and y obtained from numerical solution of Eqs. (1). Panel (a) presents a single sample, and panel (b) shows five superimposed samples of the same signal on successive time intervals. Fig. (b) gives evidence that the process is not periodic. Chaos manifests itself in irregular displacement of maxima and minima of the waveforms relative to the envelope on successive time intervals T.

To have a quantitative indicator of chaos we turn to Lyapunov exponents. With multiple iterations of the Poincaré map and Jacobi matrix computations, we trace evolution of four perturbation vectors by means of their subsequent multiplication by the Jacobi matrices. At each iteration, the Gram – Schmidt orthogonalization and normalization are performed for the set of vectors. The Lyapunov exponents are determined as the mean rates for growth or decrease of the accumulating sums for logarithms of norms for the vectors (after orthogonalization but before the normalization) [21]. From the computations (10 samples, each of $5 \cdot 10^4$ iterations of the Poincaré map) we obtained the Lyapunov exponents

$$\begin{array}{ll} L_1 = 0.6832 \pm 0.0007, & L_2 = -2.6022 \pm 0.0036, \\ L_3 = -4.6054 \pm 0.0028, & L_4 = -6.5381 \pm 0.0078. \end{array} \tag{13}$$

Presence of the positive exponent L_1 indicates chaos. (It is close to $\ln 2 = 0.6931$ because of applicability of the approximate Bernoulli map (4).)

Figure 6 shows portraits of the attractor on a plane of variables of the first oscillator. The panel (a) depicts projection of the attractor from the 5D extended phase space on the plane of original variables (x, u). The attractor is shown in gray scales (the darkness reflects a relative duration of residence inside a given pixel). Black dots relate to the Poincaré cross-section, the instants $t_n = nT$. The panel (b) shows the attractor in the Poincaré cross-section on a plane of the redefined coordinates (x_0, x_1) (see (5)). Note an evident visual similarity with the Smale – Williams attractor as depicted in textbooks. The transverse Cantor-like structure is illustrated separately on the panels (c) and (d). For quantitative characterization of the fractal structure in the Poincaré cross-section, we estimated the correlation dimension by means of the algorithm of Grassberger and Procaccia. Using a 4-component time series $\mathbf{x}_n = \mathbf{x}(t_n)$ obtained from numerical iterations of the Poincaré map for n=1÷M, M=40000, we get

D=1.2516±0.0018 (as a result of averaging over 10 samples). The dimension estimated from Luapunov exponents with the Kaplan – Yorke formula is $D \approx 1.263$.

From the point of view of theoretical analysis of the hyperbolic attractors, one of the principal features is that intersections of the stable and unstable manifolds if occur must be transversal. In computations, to determine the manifolds with appropriate accuracy one can use the following scheme. Let us have three points on the attractor obtained one from another by N-fold application of the Poincaré map: $\mathbf{x}_A \to \mathbf{x}_B = \mathbf{T}^N(\mathbf{x}_A) \to \mathbf{x}_C = \mathbf{T}^N(\mathbf{x}_B)$, where N is a sufficiently large integer. To obtain the 1D unstable manifold at B, we consider an ensemble of initial conditions close to A and parametrized by $\Delta\psi$, a small deflection of the angle variable, of order L_1^{-N}: $x_0 = r^A \sin\psi$, $x_1 = r^A \cos\psi$, $x_2 = x_2^A$, $x_3 = x_3^A$, $r^A = \sqrt{(x_0^A)^2 + (x_1^A)^2}$, $\psi = \psi^A + \Delta\psi$, $\psi^A = \arg(x_1^A + ix_0^A)$. After N iterations of the map $\mathbf{T}$, the points take up positions along the unstable manifold Γ_u^B. To obtain the 3D stable manifold at B we set initial conditions for the Poincaré map close to B: $x_0 = (r^B + \Delta r)\sin\psi_0$, $x_1 = (r^B + \Delta r)\cos\psi_0$, $x_2 = x_2^B + \Delta x_2$, $x_3 = x_3^B + \Delta x_3$, where $r^B = \sqrt{(x_0^B)^2 + (x_1^B)^2}$. Fixing three values ($\Delta r$, Δx_2, Δx_3), which parametrize the manifold, we take as initial guess $\psi_0 = \psi^B = \arg(x_1^B + ix_0^B)$ and perform N iterations of the map. Then, we get a discrepancy $\psi_N - \psi^C$, $\psi^C = \arg(x_1^C + ix_0^C)$, correct the initial angle variable, $\psi_0' = \psi_0 + (\psi^C - \psi_N)/2^N$, and repeat the procedure, until the error will be less than a given small value.

A graphic representation of the manifolds is not trivial because the phase space is four-dimensional. Let us use a plane of variables (x_0, x_1) relating to the first oscillator. The 1D unstable manifold may be shown simply as a projection onto this plane. For representation of a 3D stable manifold we use a curve of intersection of the manifold with the 2D plane $\{x_2 = x_2^B,\ x_3 = x_3^B\}$ projected onto the plane (x_0, x_1). Practically, a sufficient accuracy for coordinates of points on the manifolds is reached, say, at $N \sim 10$. The disposition of the local manifolds revealed from the computations is illustrated in Fig. 7. The invariant set that consists of the unstable manifolds coincides with the attractor itself. It is enclosed in the toroidal absorbing domain going turn by turn around "the hole of the doughnut". On the other hand, the stable manifolds are posed across the "tube" that forms a surface of the toroid. In the two-dimensional diagram the stable manifolds look like "speaks of a wheel". Due to such mutual location, the stable and unstable manifolds can intersect only transversally, and no tangencies do occur.

As stated in this article, in the 4D phase space of Poincaré map for the system of two non-autonomous coupled van der Pol oscillators there exists a toroidal absorbing domain, containing a uniformly hyperbolic attractor. This conclusion is based on computer verification of conditions formulated in terms of inclusions for expanding and contracting cones defined in the tangent vector spaces associated with the points of

the absorbing domain. Hence, our model delivers a long-time expected example of a simple physically realistic system with a hyperbolic attractor of the Smale–Williams type. With this example, it will be possible to construct other models with hyperbolic chaos, exploiting structural stability of the hyperbolic attractors. In fact, a physical experiment demonstrating attractor of this type has been performed already on a basis of coupled electronic oscillators [16]. In applications, the systems with hyperbolic chaos may be of special interest because of their robustness (structural stability). An interesting, and now a substantial direction is constructing chains, lattices, networks on a base of elements with hyperbolic chaos [22]. Models of this class may be of interest for understanding deep and fundamental questions, like the problem of turbulence.

This research was supported by RFBR grant No 06-02-16619.

References

[1] Ya.G. Sinai, in: Nonlinear Waves. Ed. A.V. Gaponov – Grekhov (Nauka Moscow 1979) 192 (in Russian).

[2] J.-P. Eckmann and D. Ruelle, Rev. Mod. Phys. **57** (1985) 617.

[3] R.L. Devaney, An Introduction to Chaotic Dynamical Systems (Addison-Wesley, New York, 1989).

[4] L. Shilnikov, Int. J. of Bifurcation and Chaos **7** (1997) 1353-2001.

[5] A. Katok and B. Hasselblatt, Introduction to the Modern Theory of Dynamical Systems. (Cambridge: Cambridge University Press, 1995).

[6] V. Afraimovich and S.-B. Hsu, Lectures on chaotic dynamical systems, AMS/IP Studies in Advanced Mathematics, **28**, American Mathematical Society, Providence, RI; International Press, Somerville, MA (2003).

[7] E. Ott, Chaos in Dynamical Systems (Cambridge University Press, 1993).

[8] V.S. Anishchenko, V.V. Astakhov, A.B. Neiman, T.E. Vadivasova, and L. Schimansky-Geier, Nonlinear Dynamics of Chaotic and Stochastic Systems. Tutorial and Modern Development (Springer, Berlin, Heidelberg, 2002).

[9] V.S. Afraimovich, V.V. Bykov, and L.P. Shil'nikov, Sov. Phys. Dokl. **22** (1977) 253.

[10] K. Mischaikow and M. Mrozek, Bull. Am. Math. Soc. **32** (1995) 66.

[11] T.J. Hunt and R.S. MacKay, Nonlinearity **16** (2003) 1499.

[12] T.J. Hunt, PhD Thesis, Univ. of Cambridge (2000).

[13] V. Belykh, I. Belykh and E. Mosekilde, Int. J. of Bifurcation and Chaos **15** (2005) 3567.

[14] L.P. Shil'nikov and D.V. Turaev, Doklady RAS **342** (1995) 596 (in Russian).

[15] S.P. Kuznetsov, Phys. Rev. Lett. **95** (2005) 144101.

[16] S.P. Kuznetsov and E.P. Seleznev, JETP **102** (2006) 355.

[17] V.I. Arnol'd, Ordinary Differential Equations (Springer-Verlag, Berlin,1992).

[18] A.A. Andronov, A.A. Vitt, S.E. Khaikin, Theory of Oscillators (Dover Publications, New York, 1966).

[19] E. Hairer, S.P. Nørsett, and G. Wanner, Solving Ordinary Differential Equations I. (Springer Verlag, 1993).

[20] LAPACK, version 3.0: http://www.netlib.org/lapack (2000).

[21] G. Benettin, L. Galgani, A. Giorgilli, J.-M. Strelcyn, Meccanica, **15** (1980) 9.

[22] L.A. Bunimovich and Ya.G. Sinai, Nonlinearity, **1** (1988) 491.

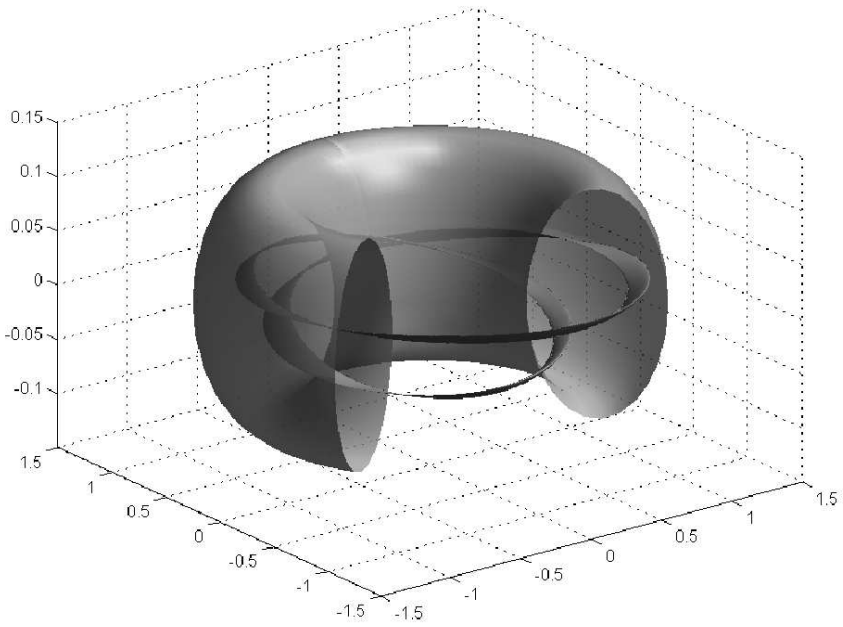

Figure 1: The toroidal absorbing domain U and its image $\mathbf{T}(U)$ shown in a 3D projection. Variables x_0, x_1 are plotted along the axes in the horizontal plane, and x_2 along the vertical axis. The fourth variable x_3 corresponds to direction of the projecting.

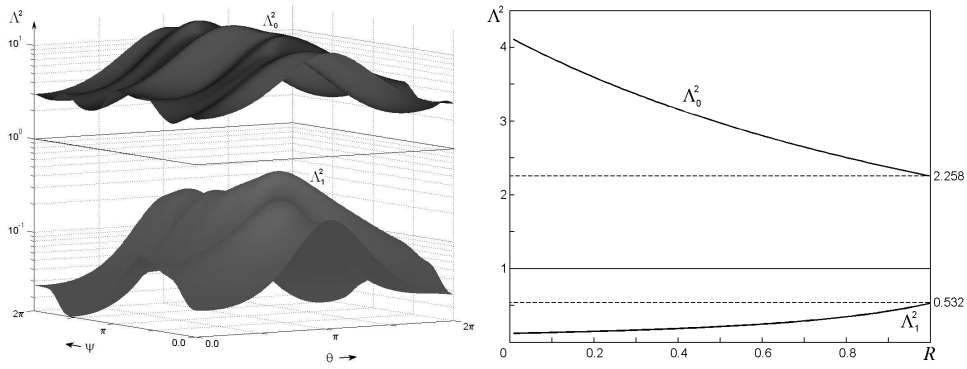

Figure 2: Eigenvalues Λ_0^2 and Λ_1^2 in dependence on the angle coordinates ψ and θ at $R = 1$ and ϕ =const (a) and dependences of the global minimum for Λ_0^2 and global minimum for Λ_1^2 over three variables ϕ, ψ, θ versus parameter R (b).

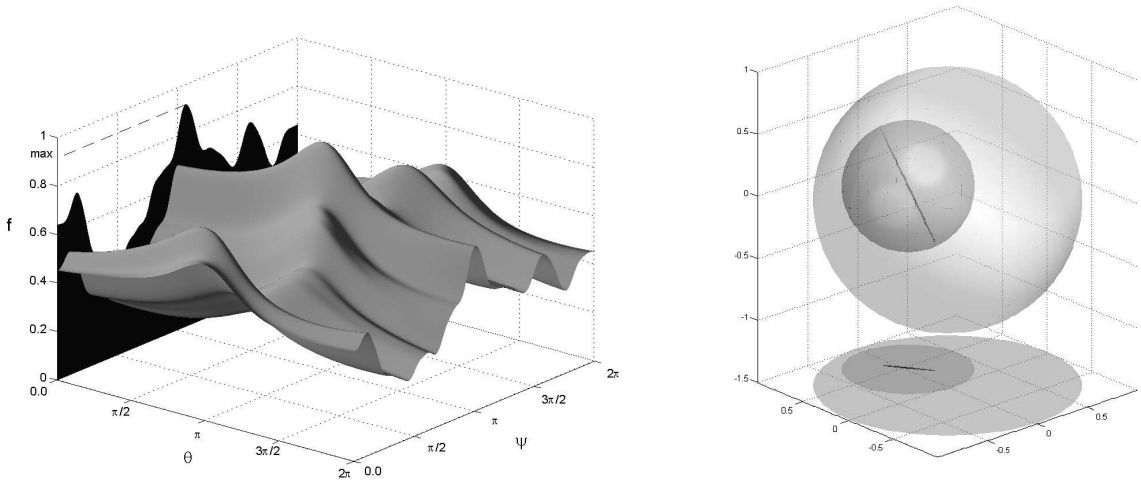

(a) (b)

Figure 3: A plot of the function $r_{\max} + \rho = f(R, \phi, \psi, \theta)$ at $R = 1$ and $\phi = 1.25665$ with $\gamma^2 = 1.1$ (a) and a diagram illustrating mutual disposition of the 3D cross-sections of the cones $\mathbf{DT_x}(S_{\mathbf{x}}^{\gamma})$ and $S_{\mathbf{T(x)}}^{\gamma}$ at the point of global maximum of $r_{\max} + \rho$.

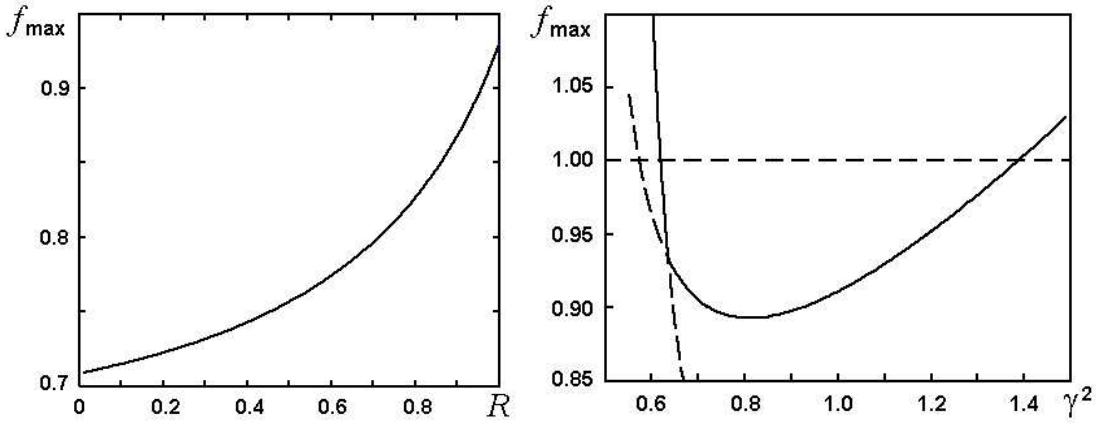

Figure 4: Value of the global maximum of the function $f = r_{\max} + \rho$ on a hypersurface (11) versus parameter R (a) and the global maximum value over the whole absorbing domain U in dependence on parameter γ.

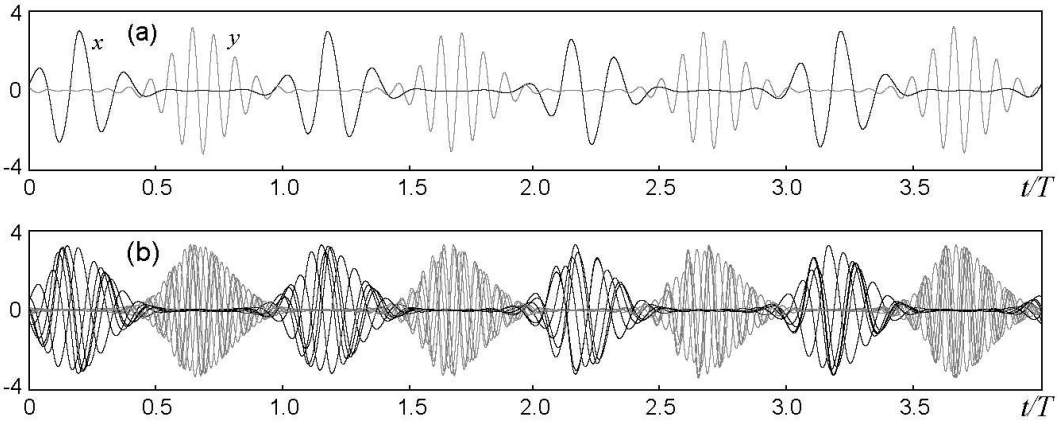

Figure 5: Typical patterns of time dependences for the variables x and y obtained from numerical solution of Eqs. (1) at $T = 6$, $A = 5$, $\varepsilon = 0.5$. Panel (a) presents a single sample, and panel (b) shows five superimposed samples of the same signal on successive time intervals.

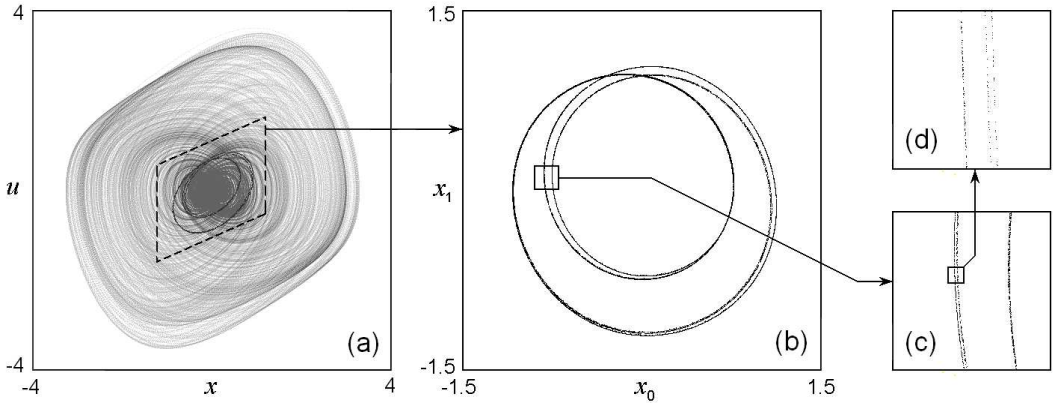

Figure 6: Portraits of the attractor on a plane of variables of the first oscillator: (a) – projection of the attractor from the 5D extended phase space on the plane of original variables (x, u); (b) – the attractor in the Poincaré cross-section on a plane of the redefined coordinates (5); (c), (d) – details of the Cantor-like transverse structure.

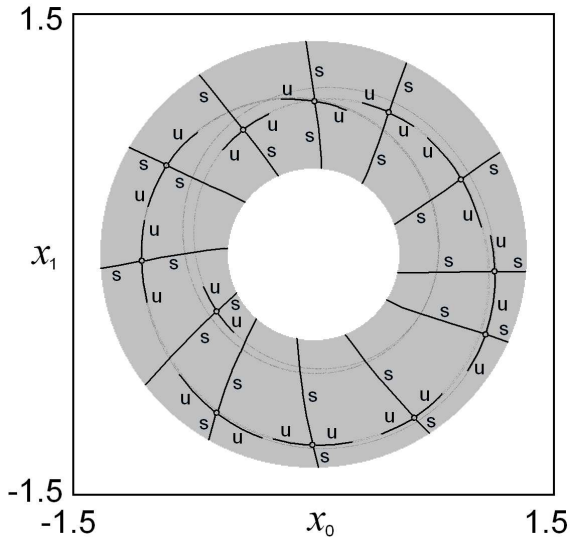

Figure 7: A diagram on the plane of variables (x_0, x_1) illustrating mutual location of local unstable (u) and stable (s) manifolds for a set of points on the attractor in the Poincare cross-section. The gray ring-shaped area depicts a projection of the absorbing domain U.